Using inherited cosmogenic ^{36}Cl to constrain glacial erosion rates of the Cordilleran ice sheet

Jason P. Briner*
Terry W. Swanson
Department of Geological Sciences and Quaternary Research Center,
University of Washington, Box 351310, Seattle, Washington 98195

ABSTRACT

Cosmogenic ^{36}Cl/Cl ratios measured from glacially eroded bedrock provide the first quantitative constraints on the magnitude, rate, and spatial distribution of glacial erosion over the last glacial cycle. Of 23 ^{36}Cl/Cl ratios, 8 yield exposure ages that predate the well-constrained deglaciation of the Puget Lowland, Washington, and are inferred to result from ^{36}Cl inherited from prior exposure during the last interglaciation where ice did not erode enough rock (~1.80–2.95 m) to reset ^{36}Cl/Cl ratios to background levels. Surfaces possessing inherited ^{36}Cl evidently were abraded only 0.25–1.06 m, corresponding to abrasion rates of 0.09–0.35 mm·yr^{-1}. These results indicate that in the absence of glacial quarrying, the Cordilleran ice sheet may have abraded as little as 1–2 m of bedrock near its equilibrium-line altitude over the last glacial cycle, equating to only tens of meters over the entire Quaternary.

INTRODUCTION

Although many researchers have discussed the glacial origin of stoss-and-lee topography (e.g., Jahns, 1943; Hallet, 1979), only Jahns (1943) attempted to determine quantitative estimates of glacial erosion by using exfoliation patterns in granitic domes that were differentially eroded by the Laurentide ice sheet during the last glaciation. Jahns's study provided some general constraints regarding differential erosion of stoss-and-lee features, but the relative importance of glacial quarrying vs. abrasion, as well as the magnitude and rate of erosion by continental ice sheets, is essentially unknown (Sugden et al., 1992; Hallet, 1996).

Over the past decade, cosmogenic nuclides (i.e., ^{3}He, ^{10}Be, ^{21}Ne, ^{26}Al, and ^{36}Cl) have been used successfully as geochronometers on a variety of geologic surfaces (Nishiizumi et al., 1989; Zreda et al., 1991). Researchers have also used these nuclides to address a number of erosion problems (e.g., Liu et al., 1994, 1996). As a result, the complexities of each isotopic system have become better understood. The multiple production pathways of ^{36}Cl make it particularly useful for addressing geomorphic problems related to non-quartz-bearing rocks.

COSMOGENIC ^{36}Cl PRODUCTION

Cosmogenic ^{36}Cl is produced at the Earth's surface through four different reaction pathways (Fabryka-Martin, 1988). Two involve spallogenic reactions with ^{39}K and ^{40}Ca, another involves thermal neutron activation of ^{35}Cl, and a fourth involves muon capture by ^{40}Ca, which only accounts for up to 9% of total ^{36}Cl production for calcic rocks (Stone et al., 1996). For various rock compositions in which production ranged from purely spallogenic to purely thermal neutron activation, production vs. depth profiles were calculated by Liu et al. (1994) using a calculated attenuation length of 170 ± 13 g·cm^{-2}. The depth at which spallogenic ^{36}Cl/Cl ratios is equal to background ratios (three attenuation lengths) is ~2 m. Extrapolating from Liu et al.'s (1994) thermal neutron depth profiles through the use of an exponential decrease in production below 100 g·cm^{-2}, we calculate that ~3 m is the depth at which the thermally produced ^{36}Cl/Cl ratio is equal to accelerator mass spectrometry (AMS) background levels.

Where independent age control constrains the timing of surface exposure following a given geomorphic event, such as a glaciation, ^{36}Cl concentrations that are higher than expected can be inferred to reflect ^{36}Cl inherited from prior exposure, presumably attributable to a lack of sufficient glacial erosion to remove the surface rock in which ^{36}Cl accumulated prior to glaciation. Under such circumstances, it is possible to constrain the magnitude of glacial erosion, provided that postglacial erosion rates are known or negligible and the preglacial exposure history of the geomorphic surface is inferred correctly.

RESEARCH MOTIVATION AND DESIGN

The advance and retreat of the Cordilleran ice sheet during the last (Fraser) glaciation in the northern Puget Lowland are well delimited between ca. 18 to 15 (calendar) ka (Stuiver and Reimer, 1993; Bard et al., 1993) by numerous ^{14}C ages from organic material that underlies, is found within, and overlies Fraser glacial deposits (Clague et al., 1988; Swanson, 1994). Swanson (1994) sampled more than 60 glacial-erratic boulders and abraded bedrock surfaces (mean surface age 15.2 ± 0.7 [calendar] ka) in the northern Puget Lowland in an effort to calibrate the ^{36}Cl production rates. In this study, two anomalously old ^{36}Cl model ages of 32.8 ± 1.6 and 33.2 ± 1.45 ^{36}Cl ka (the term ^{36}Cl or ^{36}Cl ka is used to describe surface exposure ages based on the ^{36}Cl isotopic system and is calibrated to the ^{14}C chronology of the deglaciation history of the northern Puget Sound region, Washington) were obtained from abraded surfaces near the summit of Mount Erie, a large stoss-and-lee landform located in the northern Puget Lowland (Fig. 1A). These excessive ^{36}Cl model ages are attributed to inherited ^{36}Cl atoms that accumulated prior to the last glaciation and were preserved owing to minimal glacial erosion of the upper ~2–3 m of rock. This initial finding motivated us to assess the magnitude, rate, and spatial distribution of glacial erosion on this stoss-and-lee landform by using the ^{36}Cl method. To complete these objectives, we have used the modified ^{36}Cl production rates of Swanson (1994), which were calibrated in the same general location as the Mount Erie samples; consequently, error associated with incorrect latitudinal scaling factors and time integrated paleomagnetic field intensity changes is minor. Moreover, independent dating control for this calibration location is very well constrained.

Mount Erie (388 m altitude) is ~300 m higher than the surrounding topography and is composed of highly resistant, fractured gabbroic rock. During the time of maximum extent of the Cordilleran ice sheet, Mount Erie

---

*Present address: Department of Geology, Utah State University, Logan, Utah 84322. E-mail: SL04V@cc.usu.edu.

Data Repository item 9807 contains additional material related to this article.

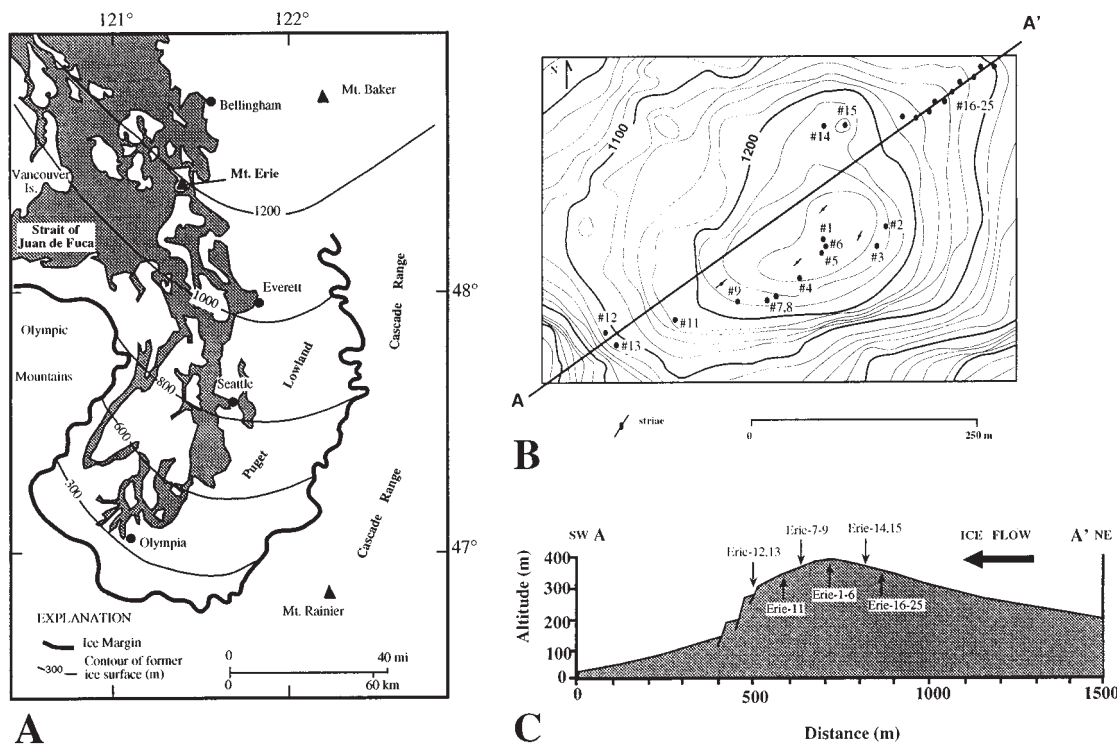*Geology;* January 1998; v. 26; no. 1; p. 3–6; 3 figures; 1 table.

3

Figure 1. A: Map of Puget Lowland showing Mount Erie in relation to maximum extent of Puget lobe during Fraser glaciation (modified from Booth, 1986). B: Plan view of summit region of Mount Erie showing sample localities. Samples 1–6 are from nearly horizontal surfaces at and near summit; 7–9 and 11 are from abraded lee surfaces; 12 and 13 were taken from quarried lee surfaces; and 14–25 are from stoss-side surfaces with varying dip angles that range from 0° to 30°. Insufficient amounts of Cl were extracted from samples 10 and 22. C: Stoss-to-lee cross section showing sample localities. Ice-flow direction is from northeast to southwest, as indicated by glacial groove and striae orientations.

was approximately at the equilibrium line where ice attained a thickness of 1200–1500 m and basal ice velocities were ≥ 500 m · yr^{-1} (Booth, 1986). The mountain is a stoss-and-lee landform with a steep south- to southwest-facing lee slope and a gently dipping. north- to northeast-facing stoss slope (Fig. 1, B and C). Signs of abrasion on stoss sides of these features include striae, polish, and grooves; evidence of quarrying is seen in 1–2-m-high vertical lee surfaces. The lee side exhibits a stepped topography with "risers" ranging from 5 to 10 m (Fig. 1C). The pattern and spatial distribution of abrasion and quarrying are clear and tend to be strongly linked with west-northwest–trending fracture patterns.

We collected 25 rock samples from the upper 1 cm of glacially abraded, polished, and quarried surfaces along a stoss-to-lee transect (Fig. 1, B and C). For most of our samples, correction for topographic shielding was <1%. Abundant polished and striated surfaces indicate that Mount Erie has undergone negligible weathering since deglaciation. Chlorine was extracted from rock samples by using a wet-chemical technique modified from Zreda et al. (1991). ^{36}Cl/Cl ratios were measured by AMS at the Lawrence Livermore National Laboratory, Livermore, California. Major and trace elements were measured using standard geological methods.

^{36}Cl ages range from the timing of deglaciation to 37 ka (^{36}Cl) (Table 1; see Appendix 1[1] for a complete list of major element compositions). Eight samples predate deglaciation (15 [calendar] ka) by at least 5 k.y. (^{36}Cl) (~3σ above the mean and individual sample error) and are inferred to contain inherited preglacial ^{36}Cl in addition to ^{36}Cl that has accumulated since deglaciation, thereby yielding older exposure ages.

CONSTRAINTS ON GLACIAL EROSION

To constrain magnitudes of erosion, it is necessary to determine the depth at which ^{36}Cl production is less than or equal to 1σ analytical uncertainty (~5%). For Mount Erie's gabbro (density of 2.8 g · cm^{-2}), the depth equal to one attenuation length is ~61 cm. For a sample whose ^{36}Cl production results entirely from spallation reactions, the amount of ^{36}Cl produced is equal to or less than the measurement error at about three attenua-

tion lengths, or 183 cm (Fig. 2). For a sample whose ^{36}Cl production results entirely from thermal neutron activation, the depth at which ^{36}Cl production is less than or equal to measurement error is ~2.95 m (Fig. 2). These depths were calculated for each of our samples and range from 1.89 m for a sample with 92% spallogenically produced ^{36}Cl to 2.37 m for a sample with only 50% spallogenically produced ^{36}Cl (Table 1). From these calculated depths it is possible to determine constraints on the magnitudes of erosion, which are minimums for samples without inherited ^{36}Cl (i.e., age of deglaciation) and maximums for the eight samples that contain inherited ^{36}Cl (Table 1).

Depths of erosion are calculated for samples possessing inherited ^{36}Cl by using a spreadsheet program that models ^{36}Cl concentration vs. depth over time. The model uses depth-profile data from Liu et al. (1994) and assumes an exponential decrease in ^{36}Cl production for the thermal component below 100 g · cm^{-2}. If a conservative postglacial erosion rate of 1 mm · k.y.$^{-1}$ is used, the concentration of ^{36}Cl required to yield the age of deglaciation is calculated for each sample by using the ^{36}Cl production rates of Swanson (1994) and latitudinal and altitudinal scaling factors reported by Lal (1991). The inherited component of ^{36}Cl concentration at deglaciation is determined by subtracting the calculated ^{36}Cl (with the assumption of 15 [calendar] k.y. of production and decay since deglaciation) from the measured ^{36}Cl concentrations (Table 1).

Two assumptions are necessary to calculate the magnitude of glacial erosion for those surfaces possessing inherited ^{36}Cl. First, it is assumed that the preglacial erosion rate at the summit of Mount Erie was the same as the postglacial erosion rate. Palynological data indicate that climatic conditions during stage 3 were slightly cooler than at present in the Puget Lowland (Hansen and Easterbrook, 1974). Second, the starting point for ^{36}Cl accumulation of inherited samples is inferred to be ca. 70 ka, near the start of the Possession deglaciation (marine oxygen isotope stage 4) when the Puget lobe of the Cordilleran ice sheet terminated south of Mount Erie (Clague et al., 1992). It is unlikely that much, if any, inherited ^{36}Cl would exist from the last interglaciation (stage 5) because only a small proportion of our samples (one-third) contain inherited ^{36}Cl today. Furthermore, the upglacier migration of quarried surfaces during successive glaciations would ultimately result in little preservation of inherited ^{36}Cl. Consequently, ice cover

---

[1]Data Repository item 9807, Appendix 1, is available on request from Documents Secretary, GSA, P.O. Box 9140, Boulder, CO 80301.

Sample no.	³⁶Cl/Cl ratio* (X10⁻¹⁵)	Calculated age (³⁶Cl)†	% of ³⁶Cl inherited‡	% spallogenic	Min depth of erosion (m; P ≈ 5%)•	Max depth of erosion (m; P ≈ 5%)**	Erosion rate (mm/yr) min	Erosion rate (mm/yr) max	Modeled erosion depth (cm)††	Modeled abrasion rate (mm/yr)
1	283 ± 8.63	11.4 ± 0.86	-31.58	87.6	1.94 ± 0.09		0.65 ± 0.03			
2	223 ± 6.18	13.6 ± 0.92	-10.29	80.1	2.03 ± 0.08		0.68 ± 0.03			
3	208 ± 5.7	14.2 ± 1.10	-5.63	74.5	2.09 ± 0.11		0.70 ± 0.04			
4	154 ± 2.99	17.1 ± 1.10	12.28	67.7	2.17 ± 0.10		0.72 ± 0.03			
5	155 ± 4.57	13.9 ± 1.03	-7.91	72.0	2.12 ± 0.10		0.71 ± 0.03			
6	596 ± 2.89	12.9 ± 0.88	-16.28	92.3	1.89 ± 0.10		0.63 ± 0.03			
7	233 ± 7.86	26.5 ± 2.09	43.40	66.1		2.19 ± 0.10		0.73 ± 0.03	84.0 ± 3.81	0.28 ± 0.01
8	314 ± 6.15	33.2 ± 2.48	54.82	69.4		2.15 ± 0.12		0.72 ± 0.04	38.0 ± 2.10	0.13 ± 0.01
9	275 ± 5.31	36.8 ± 2.37	59.24	64.2		2.21 ± 0.10		0.74 ± 0.03	55.0 ± 2.49	0.18 ± 0.01
10	no Cl extracted									
11	232 ± 8.34	19 ± 1.54	21.05	73.6	2.10 ± 0.08		0.70 ± 0.03			
12	103 ± 2.93	14 ± 1.18	-7.14	62.5	2.23 ± 0.10		0.74 ± 0.03			
13	196 ± 9.5	14.1 ± 1.18	-6.38	79.9	2.03 ± 0.11		0.68 ± 0.04			
14	155 ± 3.77	17.1 ± 1.27	12.28	67.0	2.18 ± 0.08		0.73 ± 0.03			
15	323 ± 11	37 ± 2.74	59.46	72.7		2.11 ± 0.11		0.70 ± 0.04	26.5 ± 1.33	0.09 ± 0.00
16	155 ± 4.12	16.1 ± 1.70	6.83	66.9	2.18 ± 0.09		0.73 ± 0.03			
17	257 ± 6.92	23 ± 0.74	34.78	65.9		2.19 ± 0.18		0.73 ± 0.06	87.0 ± 6.98	0.29 ± 0.02
18	443 ± 11.8	29.6 ± 2.43	49.32	73.6		2.10 ± 0.01		0.70 ± 0.00	72.5 ± 0.38	0.24 ± 0.00
19	431 ± 7.95	32.5 ± 2.06	53.85	78.5		2.05 ± 0.11		0.68 ± 0.04	62.5 ± 3.45	0.21 ± 0.01
20	435 ± 11.6	19.4 ± 1.29	22.68	87.7	1.94 ± 0.09		0.65 ± 0.03			
21	113 ± 3.35	18.5 ± 1.29	18.92	50.1	2.37 ± 0.10		0.79 ± 0.03			
22	no Cl extracted									
23	187 ± 5.6	20.3 ± 1.72	26.11	70.1		2.14 ± 0.09		0.71 ± 0.03	106 ± 4.27	0.35 ± 0.01
24	383 ± 9.89	17.7 ± 0.46	15.25	90.0	1.92 ± 0.11		0.64 ± 0.04			
25	181 ± 4.38	15.9 ± 0.38	5.66	73.3	2.11 ± 0.12		0.70 ± 0.04			

*³⁶Cl/Cl ratios ± AMS uncertainty measured at Lawrence Livermore National Laboratory, Livermore, California.
†Reported error of calculated ages includes AMS and total Cl uncertainty.
‡Percentage of inherited ³⁶Cl equals the measured concentration minus the modeled concentration at deglaciation.
•Minimum depth of erosion can be calculated for those samples for which the measured ³⁶Cl concentrations yield deglaciation ages. P is ³⁶Cl production
**Maximum depth of erosion can be calculated for samples with inherited ³⁶Cl. P is ³⁶Cl production
††Reported uncertainty includes AMS and total Cl error (geologic uncertainties are discussed in text).

over this region during the last two glaciations would likely have eroded enough rock to remove ³⁶Cl inherited from the last interglaciation.

The magnitude of glacial erosion can be obtained for each sample by modeling the ³⁶Cl concentration vs. depth that would exist at the time of deglaciation. To determine this modeled depth profile, ³⁶Cl atoms are allowed to accumulate from the starting point (ca. 70 ka) to the onset of glaciation at Mount Erie (ca. 18 ka); then they decay without further accumulation during the ca. 3 (calendar) k.y. the ice sheet shielded Mount Erie. As shown in Figure 3, the depth of erosion equals that point on the depth profile that corresponds to the calculated inherited ³⁶Cl atoms.

Eight samples containing inherited ³⁶Cl indicate magnitudes of erosion that range from 26.5 to 106 cm. These values reflect abrasion rates that range from 0.09–0.35 mm · yr⁻¹ (Table 1) for ~3 (calendar) k.y. of ice cover,
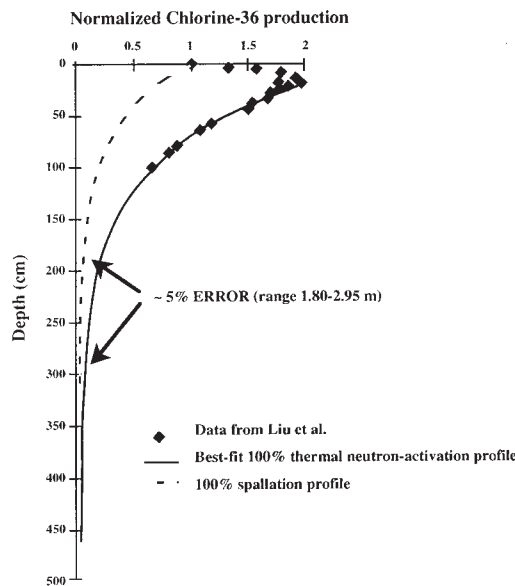

Figure 2. Normalized ³⁶Cl production vs. depth profiles for 100% spallation of ³⁹K and ⁴⁰Ca and for 100% thermal neutron activation of ³⁶Cl. Best-fit exponential decay curve is used for thermal neutron activation profile to extend curve beyond measured data of Liu et al. (1994). As result of accelerator mass spectrometry (AMS) uncertainty, measured ³⁶Cl concentrations cannot be detected at depths beyond where production is <5% of surface production. This AMS uncertainty (~5%) equates to depths of 1.80 and 2.95 m for 100% spallation and 100% thermal neutron activation samples, respectively.
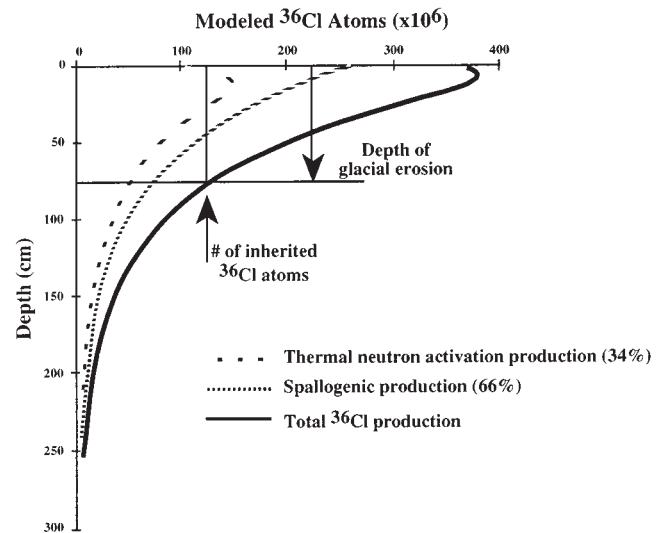

Figure 3. Modeled ³⁶Cl concentration vs. depth profile for sample 7 at onset of deglaciation. Spallogenic (66%) and thermal neutron activation (34%) production curves add up to total production curve. Point on profile that corresponds to inherited concentration (measured concentration [column 2 in Table 1] minus modeled concentration at deglaciation [ca. 15 calendar ka]) represents depth of glacial erosion during ~3 (calendar) k.y. of ice cover.

which means as little as 3–20 m of abrasion on Mount Erie during the Quaternary. Samples without inherited ^{36}Cl only provide minimum constraints of glacial erosion and exceed 1.89 m (Table 1). Microtopographic features on Mount Erie show where quarrying was the dominant erosion mechanism. All quarried surfaces yield deglaciation ages with corresponding erosion magnitudes of >1.89–2.23 m (Table 1). All of the samples that contain inherited ^{36}Cl were collected from geomorphic surfaces that appeared nonquarried but possessed varying evidence of glacial abrasion.

The data show distinct spatial patterns of glacial erosion on Mount Erie (Table 1). The stoss side yields abrasion rates of 0.09–0.35 mm · yr^{-1}, whereas erosion rates on summit surfaces exceed 0.63–0.72 mm · yr^{-1}. Striated and polished lee surfaces 3–10 m below summit elevations and above the quarried lee region yield abrasion rates of 0.13–0.28 mm · yr^{-1}. The two samples collected from the quarried lee region yield deglaciation ages and corresponding erosion depths of ≥2 m (Table 1; Fig. 1). Because of the substantial local relief of this region, it is likely that these minimum values grossly underestimate the magnitude of glacial quarrying.

The error reported in Table 1 for the calculated ^{36}Cl ages includes 2%–5% AMS and 3%–7% total Cl measurement uncertainties because these are the dominant sources of calculated age uncertainty (Swanson, 1994). Other sources of uncertainty that could be relevant to erosion calculations include ^{36}Cl production rates (5%–7%), major and trace element measurements (<2%), and the attenuation length (~7%). Other potential sources of error that are not easily quantifiable include (1) the timing and erosive character of the Possession (stage 4) ice advance over Mount Erie, and (2) the nonglacial surface erosion rate prior to the Fraser glaciation.

The spatial variability of erosion is related to whether quarrying or abrasion was the dominant erosion process. On the downglacier side of Mount Erie, quarrying was the dominant process and ^{36}Cl ages reflect the timing of deglaciation. The low magnitudes of abrasion on the striated lee surfaces may be due to diverging ice flow downglacier from the summit where there was likely negligible coarse debris available within the basal ice to erode the bed (Rastas and Seppälä, 1981). Deglaciation ages on summit surfaces reveal that quarrying was the dominant erosion process, which is consistent with field observations. On the stoss side, inherited ^{36}Cl and striae and grooves indicate that abrasion was the dominant erosion process; however, in some locations the existence of microscale (1–2 m) stoss-and-lee features suggest that quarrying also occurred. Quarrying likely exploited preglacial joint patterns, producing a complex spatial pattern of quarried surfaces, and likely controlled local erosion rates.

CONCLUSIONS

Results from this study indicate that magnitude, rate, and spatial patterns of glacial erosion can be solved for places where both inheritance and independent age control exist. The magnitude and presence of inherited cosmogenic nuclides in glacially eroded surfaces have important implications. The low abrasion rates inferred from this study support arguments for minimal glacial erosion by continental ice sheets in geomorphic settings where glacial quarrying is absent and/or locations where bedrock lithology is highly resistant to abrasion. Furthermore, the results presented herein demonstrate the potential that cosmogenic nuclide studies may have in resolving research questions relevant to glacial erosion processes, such as testing existing theories of glacial abrasion and quarrying (e.g., Sugden et al., 1992; Hallet, 1996).

Glacial chronologies based on cosmogenic dating techniques may be inaccurate if dated surfaces within the study area contain inherited nuclides. Glacially abraded surfaces have been used in a number of studies to constrain the rates of cosmogenic nuclide production (e.g., Nishiizumi et al., 1989; Zreda et al., 1991; Swanson, 1994). The data presented here indicate that exposure ages of some glacially abraded surfaces may not truly represent the timing of deglaciation because of unknown inheritance. This factor may be most problematic for geomorphic settings where there is little erosion (i.e., unconstricted ice flowing over resistant bedrock lithologies, a very

short period of ice cover, or under cold-based ice). The inheritance of cosmogenic nuclides may therefore be significant and must be considered when estimating ages of glacially eroded bedrock.

REFERENCES CITED

Bard, E., Arnold, M., Fairbanks, R. G., and Hamelin, B., 1993, ^{230}Th-^{234}U and ^{14}C ages obtained by mass spectrometry on corals: Radiocarbon, v. 35, p. 191–199.

Booth, D. B., 1986, Mass balance and sliding velocity of the Puget lobe of the Cordilleran ice sheet during the last glaciation: Quaternary Research, v. 25, p. 269–280.

Clague, J. J., Saunders, I. R., and Roberts, M. C., 1988, Ice-free conditions in southwestern British Columbia at 16,000 years B.P.: Canadian Journal of Earth Sciences, v. 25, p. 938–941.

Clague, J. J., Easterbrook, D. J., Hughes, O. L., and Mathews, J. V., 1992, The Sangamonian and early Wisconsinan stages in western Canada and northwestern United States, in Clark, P. U., and Lea, P. D., eds., The last interglacial-glacial transition in North America: Geological Society of America Special Paper 270, p. 253–268.

Fabryka-Martin, J. T., 1988, Production of radionuclides in the Earth and their hydrogeologic significance with emphasis on chlorine-36 and iodine-129 [Ph.D. thesis]: Tucson, University of Arizona, 400 p.

Hallet, B., 1979, A theoretical model of glacial abrasion: Journal of Glaciology, v. 23, p. 39–50.

Hallet, B., 1996, Glacial quarrying: A simple theoretical model: Annals of Glaciology, v. 22, p. 1–8.

Hansen, B. S., and Easterbrook, D. J., 1974, Stratigraphy and palynology of late Quaternary sediments in the Puget Lowland, Washington: Geological Society of America Bulletin, v. 85, p. 587–602.

Jahns, R. H., 1943, Sheet structure in granites: Its origin and use as a measure of glacial erosion in New England: Journal of Geology, v. 51, p. 71–98.

Lal, D., 1991, Cosmic ray labeling of erosion surfaces: In situ nuclide production rates and erosion models: Earth and Planetary Science Letters, v. 104, p. 424–439.

Liu, B., Phillips, F. M., Fabryka-Martin, J. T., Fowler, M. M., and Stone, W. D., 1994, Cosmogenic ^{36}Cl accumulation in unstable landforms: 1. Effects of the thermal neutron distribution: Water Resources Research, v. 30, p. 3115–3125.

Liu, B., Phillips, F. M., Pohl, M. M., and Sharma, P., 1996, An alluvial surface chronology based on cosmogenic ^{36}Cl dating, Ajo Mountains (Organ Pipe Cactus National Monument), southern Arizona: Quaternary Research, v. 45, p. 30–37.

Nishiizumi, K., Winterer, E. L., Kohl, C. P., Klein, J., Middleton, R., Lal, D., and Arnold, J. R., 1989, Cosmic ray production rates of ^{10}Be and ^{26}Al in quartz from glacially polished rocks: Journal of Geophysical Research, v. 94, p. 17907–17915.

Rastas, J., and Seppälä, M., 1981, Rock jointing and abrasion forms on roches moutonnées, SW Finland: Annals of Glaciology, v. 2, p. 159–162.

Stone, J., Lambeck, K., Fifield, L. K., Evans, J. M., and Cresswell, R. G., 1996, A lateglacial age for the Main Rock Platform, western Scotland: Geology, v. 24, p. 707–710.

Stuiver, M., and Reimer, P. J., 1993, Extended ^{14}C data base and revised CALIB 3.0 ^{14}C calibration program: Radiocarbon, v. 35, p. 215–230.

Sugden, D. E., Glasser, N., and Clapperton, C. M., 1992, Evolution of large roches moutonnées: Geografiska Annaler, v. 74, p. 253–264.

Swanson, T. W., 1994, Determination of ^{36}Cl production rates from the deglaciation history of Whidbey and Fidalgo Islands, Washington [Ph.D. thesis]: Seattle, University of Washington, 118 p.

Zreda, M. G., Phillips, F. M., Kubik, P. W., Sharma, P., and Elmore, D., 1991, Cosmogenic chlorine-36 production rates in terrestrial rocks: Earth and Planetary Science Letters, v. 105, p. 94–109.